Hearing Research 371 (2019) 75–86

Contents lists available at ScienceDirect

Hearing Research

journal homepage: www.elsevier.com/locate/heares

Research Paper

Targeted single-cell electroporation loading of Ca^{2+} indicators in the mature hemicochlea preparation

Eszter Berekméri [a], Orsolya Deák [a], Tímea Téglás [a, 1], Éva Sághy [a], Tamás Horváth [a, 2], Máté Aller [a, 3], Ádám Fekete [b], László Köles [a], Tibor Zelles [a, *]

[a] Department of Pharmacology and Pharmacotherapy, Semmelweis University, Budapest, Hungary
[b] Program in Neurosciences and Mental Health, The Hospital for Sick Children, Toronto, ON, Canada

ARTICLE INFO

Article history:
Received 5 June 2018
Received in revised form
30 October 2018
Accepted 7 November 2018
Available online 10 November 2018

Keywords:
Single-cell electroporation
Ca^{2+} imaging
Hemicochlea
ATP
TRPA1
TRPV1

ABSTRACT

Ca^{2+} is an important intracellular messenger and regulator in both physiological and pathophysiological mechanisms in the hearing organ. Investigation of cellular Ca^{2+} homeostasis in the mature cochlea is hampered by the special anatomy and high vulnerability of the organ. A quick, straightforward and reliable Ca^{2+} imaging method with high spatial and temporal resolution in the mature organ of Corti is missing. Cell cultures or isolated cells do not preserve the special microenvironment and intercellular communication, while cochlear explants are excised from only a restricted portion of the organ of Corti and usually from neonatal pre-hearing murines. The hemicochlea, prepared from hearing mice allows tonotopic experimental approach on the radial perspective in the basal, middle and apical turns of the organ. We used the preparation recently for functional imaging in supporting cells of the organ of Corti after bulk loading of the Ca^{2+} indicator. However, bulk loading takes long time, is variable and non-selective, and causes the accumulation of the indicator in the extracellular space. In this study we show the improved labeling of supporting cells of the organ of Corti by targeted single-cell electroporation in mature mouse hemicochlea. Single-cell electroporation proved to be a reliable way of reducing the duration and variability of loading and allowed subcellular Ca^{2+} imaging by increasing the signal-to-noise ratio, while cell viability was retained during the experiments. We demonstrated the applicability of the method by measuring the effect of purinergic, TRPA1, TRPV1 and ACh receptor stimulation on intracellular Ca^{2+} concentration at the cellular and subcellular level. In agreement with previous results, ATP evoked reversible and repeatable Ca^{2+} transients in Deiters', Hensen's and Claudius' cells. TRPA1 and TRPV1 stimulation by AITC and capsaicin, respectively, failed to induce any Ca^{2+} response in the supporting cells, except in a single Hensen's cell in which AITC evoked transients with smaller amplitude. AITC also caused the displacement of the tissue. Carbachol, agonist of ACh receptors induced Ca^{2+} transients in about a third of Deiters' and fifth of Hensen's cells. Here we have presented a fast and cell-specific indicator loading method allowing subcellular functional Ca^{2+} imaging in supporting cells of the organ of Corti in the mature hemicochlea preparation, thus providing a straightforward tool for deciphering the poorly understood regulation of Ca^{2+} homeostasis in these cells.

Abbreviations: ACh, Acetylcholine; AITC, Allyl isothiocyanate; ATP, Adenosine triphosphate; $[Ca^{2+}]_i$, Intracellular Ca^{2+} concentration; CCD, Charge-coupled device; EGTA, Ethylene glycol-bis(2-aminoethylether)-N,N,N′,N'-tetraacetic acid; S/N, Signal-to-noise ratio; TRPA1, Transient receptor potential ankyrin repeat domain 1; TRPV1, Transient receptor potential vanilloid 1

* Corresponding author. Dept. Pharmacology and Pharmacotherapy, Semmelweis University, H-1089, Budapest, Nagyvárad tér 4, Hungary.
E-mail address: zelles.tibor@med.semmelweis-univ.hu (T. Zelles).
[1] Present/permanent address: Research Centre of Sport and Life Sciences, Budapest, Hungary.
[2] Present/permanent address: Department of Otorhinolaryngology, Head and Neck Surgery, Bajcsy-Zsilinszky Hospital, Budapest, Hungary.
[3] Present/permanent address: Computational Cognitive Neuroimaging Laboratory, Computational Neuroscience and Cognitive Robotics Centre, University of Birmingham Birmingham, UK.

https://doi.org/10.1016/j.heares.2018.11.004
0378-5955/

1. Introduction

The mammalian organ of Corti has a uniquely spiraled structure covered with bony walls in the adulthood. The special anatomy, high vulnerability and the calcification of the temporal bone makes the organ hardly attainable and hampers its investigation significantly. Therefore, most of the experimental studies in the organ of Corti are implemented in preparations made from younger animals, e.g. the explant from 3 to 5 days old (P3-5) mice or rats (Lahne and Gale, 2008; Landegger et al., 2017). At this age the organ of Corti is immature yet and the rodents are deaf, although the mechano-transducer channels are expressed and working in hair cells from P0-P2 (Fettiplace and Kim, 2014; Lelli et al., 2009; Michalski et al., 2009). The mouse and rat organ of Corti and hearing are considered to be mature both anatomically and functionally at >P15 (Ehret, 1976; Rybak et al., 1992). However, the hemicochlea preparation is available at mature stages and provides the accessibility to the organ of Corti in three different turns of the cochlea, and hence, the opportunity to investigate the cellular and molecular mechanisms of tonotopy. The preparation, preserving the delicate cytoarchitecture of the organ of Corti was originally developed for morphological, kinematic, and mechanoelectric investigations (Edge et al., 1998; He et al., 2004; Hu et al., 1999; Keiler and Richter, 2001; Richter et al., 1998). Our group was the first using it recently for real functional Ca^{2+} imaging measurements in supporting cells of the organ of Corti bulk loaded with acetoxymethyl ester conjugated (AM) Ca^{2+} indicator (Horváth et al., 2016). AM-dyes load all types of cells and allow the imaging of synchronized activity of cell groups and their intercellular communication. Bulk loading of the tissue is simple, however, takes longer time, is variable and non-selective, and causes the accumulation of the indicator in the extracellular space. In this study, we aimed at developing a novel labeling method which is faster, more selective, decreases the variability of labeling, results in lower extracellular dye spillover and light scattering from adjacent structures, and thus improves spatial resolution and reliability.

Ca^{2+} is a major intracellular second messenger (Berridge, 2016; Horváth et al., 2016; Mammano et al., 2007) and Ca^{2+} indicators are the most reliable and pervading sensors in functional imaging studies. Beside the cell permeable AM forms, small-molecule Ca^{2+} sensors are available as membrane impermeable salts. By their targeted loading into individual cells the background noise can be decreased significantly. Salt indicators can be loaded into the cell by a patch pipette via diffusion in whole-cell configuration (Beurg et al., 2009; Denk et al., 1995; Lagostena et al., 2001; Lagostena and Mammano, 2001; Lorincz et al., 2016; Zelles et al., 2006) or single-cell electroporation. Single-cell electroporation is faster, and prevents the wash-out of intracellular compounds (Nevian and Helmchen, 2007), thus does not change the physiology of the cell and does not modify the experimental results (Ishikawa et al., 2002; Vyleta and Jonas, 2014). Genetically encoded Ca^{2+} indicators are wide-spread (Horikawa, 2015) and have the advantage of being relatively selective for the cells expressing the target gene, however they are not available for every cell type and their use is not always feasible.

Glia-like supporting cells of the organ of Corti are less investigated than the receptor hair cells. Their structural, physical supporting roles are complemented with functional ones. They are important in the development, macro- and micromechanics, in sensing harmful stimuli, initiating protective mechanisms in the inner ear, and also serve as a regenerative pool for the lost hair cells (Monzack and Cunningham, 2013). Unfortunately, the majority of information on supporting cells is from studies on neonatal and young pre-hearing animals.

In this study, we set up and validated a simple, rapid and reliable method of Ca^{2+} indicator loading into individual supporting cells of the organ of Corti prepared from hearing mice. We demonstrated that the single-cell electroporation in the hemicochlea is selective to the target cell and causes little dye spillover in the extracellular space. Using this technique we were able to investigate the P2, TRPA1, TRPV1 and acetylcholine receptor (AChR) agonist-evoked cellular and subcellular dynamics of intracellular Ca^{2+} concentration in Deiters', Hensen's and Claudius' cells (DCs, HCs, CCs). The functional role of AChRs in HCs and the lack of functional role of TRPA1 and TRPV1 channels in Ca^{2+} signaling in the three supporting cell types have not been described before.

2. Materials and methods

2.1. Tissue preparation

All animal care and experimental procedures were in accordance with the National Institute of Health Guide for the Care and Use of Laboratory Animals. Procedures were approved by the Animal Use Committee of Semmelweis University, Budapest. Acutely dissected cochleae of BALB/c mice from postnatal day 15 (P15) to P21 were used. Hemicochlea preparation was carried out according to the Dallos' group method (Edge et al., 1998; Horváth et al., 2016). Briefly, mice were anesthetized superficially by isoflurane then decapitated. The head was divided in the medial plane and the cochleae were removed and placed in ice-cold modified perilymph-like solution (composition in mM: NaCl 22.5; KCl 3.5; $CaCl_2$ 1; $MgCl_2$ 1; HEPES·Na 10; Na-gluconate 120; glucose 5.55; pH 7.4; 320 mOsm/l), which was continuously oxygenated. The integrity of the preparations was assessed by the gross anatomy, location and shape of the supporting cells, hair cells, and the basal-, tectorial- and Reissner's membranes. The perilymph-like solution with reduced [Cl^-] minimizes swelling and deformation of the cochlear tissue and preserves the morphological and functional integrity of the preparation beyond 2h (Emadi, 2003; Teudt and Richter, 2007). We reduced the Cl^- influx by iso-osmotic replacement of 120 mM NaCl for Na-gluconate, a chemical efficiently used against cellular swelling in brain slice preparations, as well (Rungta et al., 2015). The medial surface of the cochlea was glued (Loctite 404, Hartford, CT) onto a plastic plate with the diameter of 7 mm. Then the cochlea was placed into the cutting chamber of a vibratome (Vibratome Series 3000, Technical Products International Inc., St. Louis, MO, USA) bathed in ice cold experimental solution and cut into two halves through the middle of the modiolus with a microtome blade moving with a 30 mm/min speed and 1 mm amplitude of vibration (Feather Microtome Blade R35, CellPath Ltd, Newtown, UK) under visual control through a stereomicroscope (Olympus SZ2-ST, Olympus Corporation, Philippines). Only the half that was glued to the plastic plate was used for imaging.

2.2. Targeted single-cell electroporation dye-loading

The method of Nevian and Helmchen in acute brain slices was adopted (Nevian and Helmchen, 2007). The experiments were performed at room temperature (22–24 °C). The hemicochleae were placed into an imaging chamber filled with the oxygenated perilymph-like solution on the microscope stage. The perfusion speed was 3.5 ml/min in the chamber. The cells were chosen in oblique illumination under a LUMPlanFl 40x/0.80w water immersion objective (Olympus, Japan) with 3.3 mm working distance. Borosilicate pipettes (5–7 MΩ) were filled with the Ca^{2+} indicators Oregon Green 488 BAPTA-1 hexapotassium salt (OGB-1) or fura-2/K^+ (ThermoFisher Scientific) dissolved in distilled water at a final concentration of 1 mM. The pipettes were mounted onto an electrode holder attached to a micromanipulator (Burleigh PCS-5000,

Thorlabs, Munich, Germany). Each chosen cell was approached and gently touched by the pipette under visual control; a single square wave current impulse of 10 ms duration and amplitude of 10 μA were sufficient to load the cells with the Ca^{2+} indicator. The pulses were generated by pCLAMP10 software-guided stimulator system (Biostim STE-7c, Supertech Ltd, Pecs, Hungary; MultiClamp 700B Amplifier and Digidata 1322A, Molecular Devices, Budapest, Hungary).

2.3. Calcium imaging

The OGB-1 dye-filled cells were illuminated by 494 ± 5 nm excitation light (Polychrome II monochromator, TILL Photonics, Germany) and the emitted light was monitored after passage through a band-pass filter (535 ± 25 nm). Fura-2/K^+ loaded cells were alternately illuminated by 340 ± 5 nm and 380 ± 5 nm excitation light and the emitted light was detected behind a 510 ± 20 nm band-pass filter. Fluorescent images were obtained with an Olympus BX50WI fluorescence microscope (Olympus, Japan) equipped with a Photometrics Quantix cooled CCD camera (Photometrics, USA). The system was controlled with the Imaging Workbench 6.0 software (INDEC BioSystems, USA). The image frame rate was 1 or 0.5 Hz during the ATP-evoked responses and 0.1 or 0.05 Hz otherwise (OGB-1 or fura-2/K^+, respectively) to reduce phototoxicity and photobleaching. Fura-2/AM was used to contrast the difference between single cell and bulk loading (Fig. 1A). The fura-2/AM loading method has been described previously (Horváth et al., 2016). Briefly, the hemicochlea was incubated with 10 μM fura-2/AM in the presence of pluronic F-127 (0.05%, w/v) for 30 min, then deesterified in standard experimental solution for 15 min before recording. The whole experiment was performed within 1.5–2 h after decapitation. Damaged cells were excluded from the study.

2.4. Drug Delivery

ATP, allyl isothiocyanate (AITC), capsaicin and carbachol (Sigma-Aldrich, USA) were added to the perfusion for 30 s. The perfusion reached the chamber in 27–30 s and the responses started in 60–80 s. The buffer volume in the perfusion chamber was about 1.9 ml. ATP, as a standard stimulus on supporting cells (Horváth et al., 2016), was always administered at the beginning and at the end of experiments to confirm the cellular responsiveness and the preparation viability. Before the first ATP application, at least a 3-min long baseline period was registered in each experiment. Minimum 10 min had to elapse between two ATP stimuli, except in the case of the Ca^{2+} free solution (composition in mM: NaCl 22.5; KCl 3.5; $MgCl_2$ 2; Hepes 10; Na-gluconate 120; glucose 5.55; EGTA 1; pH 7.4; 320 mOsm/l) when we waited at least 15 mins between two ATP applications (Horváth et al., 2016).

2.5. Data analysis

Data analysis was performed off-line. Pixel intensity within a polygonal region of interest was averaged for each frame. Fluorescence intensities were background-corrected using a nearby area devoid of loaded cells. Using OGB-1, the relative fluorescence changes were calculated as follows:

$$\frac{\Delta F}{F_0} = \frac{F_t - F_0}{F_0}$$

where F_0 is the fluorescence intensity of the baseline, and F_t is the fluorescence intensity at time t. In case of fura-2/K^+, the ratio of emitted fluorescence intensities (F_{340}/F_{380}) were calculated. The response amplitudes were defined as the maximal change in intensity. Area under curves and averages of the responses (Fig. 3) were calculated in Igor Pro 6.37.

Signal-to-noise ratio (S/N) in fura-2/AM and fura-2/K^+ loaded cells were calculated from ATP response curves of 12-12 randomly selected cells as follows:

$$\frac{S}{N} = \frac{\Delta R}{\delta_R}$$

where ΔR is the amplitude of the ATP-evoked transients and δ_R is the standard deviation of the baseline ratio prior to the ATP administration (at least 200 s).

Data are presented as mean ± standard error of the mean (SEM). The number of experiments (n) indicates the number of cells. Testing of significance ($p < 0.05$) was performed based on the distribution of the data. In case of normal distribution (tested by Shapiro-Wilk test) ANOVA, otherwise Kruskal-Wallis test were used, both followed by Bonferroni post-hoc tests. Differences were considered significant at $p < 0.05$ (*), $p < 0.01$ (**), and $p < 0.001$ (***).

3. Results

3.1. Targeted single-cell electroporation is suitable to load Ca^{2+} indicators into cells in the hemicochlea prepared from hearing mice

The organ of Corti matures during the second postnatal week of life in mice (Ehret, 1976) therefore we used P15-P21 hemicochlea preparations (Fig. 1) to investigate mature hearing (Edge et al., 1998). The preparation allowed us to image all three turns of the cochlea (Fig. 1E) and the organs of Corti were well preserved in all turns (Fig. 1A and B show an apical and a middle turn organ, respectively). The anatomical structures (e.g. membranes, stria vascularis, spiral limbus) and cells were clearly visible, identifiable and exposed to electroporation.

We optimized the electroporation described by Nevian and Helmchen (2007) for supporting cells in the hemicochlea preparation. Electroporation was fast and efficient (took 10 min overall from the positioning of the preparation in the tissue chamber under the microscope to the removal of the loading pipette, including filling of the pipette with the dye) compared to bulk loading (Fig. 1A; 30 min loading plus 15 min deesterification, Horváth et al. 2016) promoting the health of the tissue. We approached the cell, first using the manipulator under mechanical then piezoelectric control. After approaching the cells with the pipette filled with dye, we placed the tip gently on the cell membrane, and applied a 10 ms long, 10 μA square pulse to deliver the charged molecules into the somas (Fig. 2A, D, E). Forming a seal around the pipette tip by gently pushing the membrane is crucial to the selective dye injection without any spillover into the extracellular space (Fig. 1B). A single 10 ms long pulse at lower current amplitudes (2–5 μA) resulted in insufficient loading of OGB-1. Single pulses with larger currents (50–100 μA) loaded the cells with the sufficient amount of dye, but a large proportion of the cells were damaged and lost their fluorescent intensities quickly. A single 10 μA pulse could load the cells with sufficient amount of dye reliably. The cells kept their morphology and did not loose their fluorescence till the end of the experiments. Even in the case of a second loading pulse the cells survived and were responsive to stimuli. Mistargeting the pipette caused instant cellular damage and dye leakage (Supplementary Fig. 1A). The direction and speed of the loading pipette during removal was critical. A faster removal could cause the rupture of the cell membrane with consequent dye loss. Slow, fine movement preserved the cell integrity. Vertical pipette elevation gave typically the best outcome, however a diagonal pipette removal was more

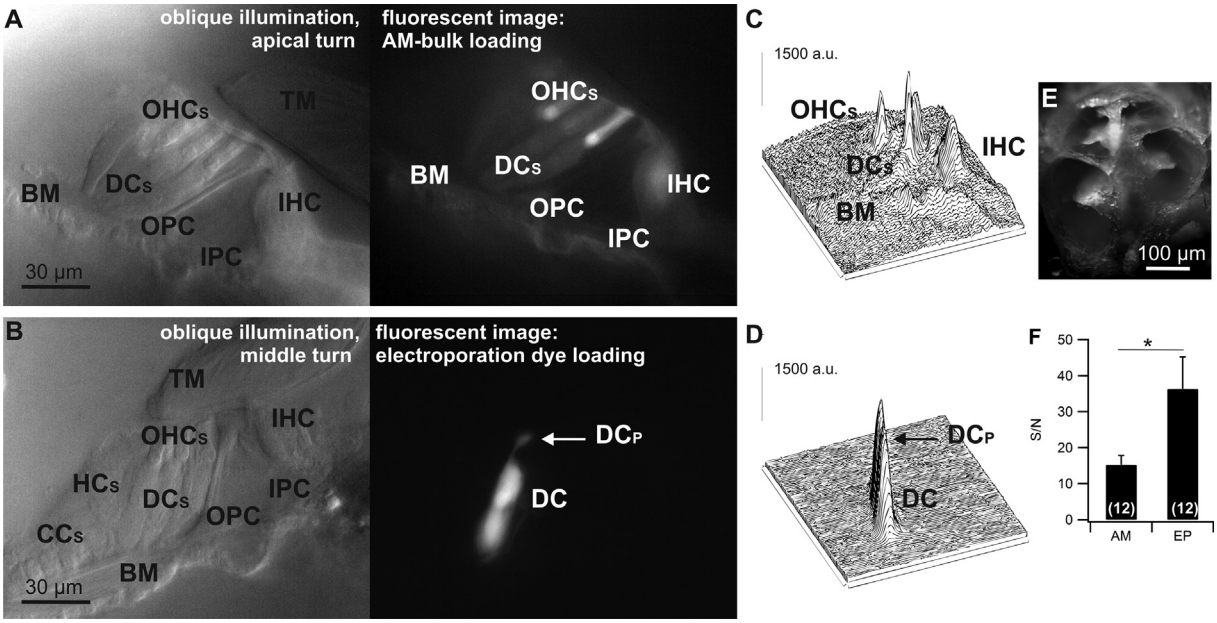

Fig. 1. Targeted single-cell electroporation provides rapid and reliable loading of fluorescent Ca^{2+} indicators in hemicochlea preparation of hearing mice. Hemicochlea preparation (E) is suitable to investigate the mature organ of Corti in different regions of the frequency map (A, B: hearing organ from the apical and the middle turn, respectively). The cells of the organ are recognizable by their location and morphology. In case of bulk loading of an AM dye (fura-2/AM) different cells took up variable amount of dye and the extracellular matrix was contaminated (A), while the single-cell electroporation of the dye (OGB-1) specifically and reliably loaded the targeted cells (B). This resulted in a significant improvement in the S/N making the stalk and the phalangeal process of the Deiters' cell visible, which is covered by the fluorescence of OHCs in case of bulk loading. Surface plot of the fluorescent images of the electroporated Deiters' cells demonstrates the low intensity of the background (D) versus the cell, while the bulk loading surface plot (Fiji analysis platform (Schindelin et al., 2012)) shows the intensity of multiple cells and the noisier background (C). S/N of ATP responses (response amplitude/standard deviation of the baseline) in 12-12 randomly selected cells loaded by fura-2/AM (bulk loading, AM) or fura-2/K^+ (electroporation, EP; F). (OHCs, outer hair cells; DCs, Deiters' cells; DCp, phalangeal process of the Deiters' cell; OPC, outer pillar cell; IPC, inner pillar cell; IHC, inner hair cell; HC, Hensen's cell; BM, basal membrane; TM, tectorial membrane).

advantageous for deeper cells.

We have not observed any punctate dye accumulation in the cytoplasm which is a sign of dye loading into the cytoplasmic organelles. However, in accord with the literature (Lagostena et al., 2001; Lagostena and Mammano, 2001) we occasionally found higher fluorescence intensity over the nucleus of the Hensen's and Claudius' cells (see Figs. 2A and 3B).

OGB-1 was tested in variable concentrations (100, 300, 500 µM and 1 mM). In the lower concentration range (100–500 µM) multiple pulses were necessary to load the cells elevating the chance of cell damage. To keep the membrane integrity we increased the dye concentration to 1 mM at which concentration a single pulse was sufficient. The pulse and the dye concentration parameters we applied for OGB-1 were appropriate for fura2/K^+ and OGB-6F (OGB-6F data are not shown).

The diffusional equilibration of the dye took approximately 5 s. A rapid loss of the intracellular fluorescence after loading indicated the damage of cell membrane (Supplementary Fig. 1A). We discarded these hemicochleae. The success rate of the targeted electroporation was ~60% and most of the loaded cells survived. The single cell loading procedure ensured the lower loading variability of supporting cells, the unambiguity of fluorescent light sources (Fig. 1B), and the decrease in dye spillover into the extracellular space (Fig. 1A and C) resulting in a significantly improved S/N compared to the bulk-loading method (Fig. 1C, D and F). These improvements together enabled us to perform subcellular imaging in the phalangeal processes of Deiters' cells in addition to their somas (Fig. 1B). The Deiters' and the Hensen's cells were easily loaded (Figs. 1B, 2A and 3B), as they are large, even in the basal turn of the cochlea where they are shorter than in the apical and middle turns (Keiler and Richter, 2001). Targeting of the laterally positioned Claudius' cells was more difficult because of their smaller size (Fig. 3B). Loading of the pillar cells was mostly unsuccessful, as their somas were too flexible to target them. Interestingly, their apical or basal part did not load through the stalk (Supplementary Fig. 1B). We could successfully load the inner and outer hair cells using the same parameters we implemented for supporting cells (Fig. 2D and E). The inner hair cell loading was more challenging because of their close contacts with the inner border and inner phalangeal cells occasionally resulting in the accidental electroporation of these supporting cells (Fig. 2E).

In order to validate the method and demonstrate its applicability in real functional imaging of receptor-mediated Ca^{2+} signaling, we tested the effect of P2, TRPA1, TRPV1 and ACh receptor stimulation. P2 purinergic Ca^{2+} signaling in supporting cells of the mature organ of Corti is well substantiated (Dulon et al., 1993; Horváth et al., 2016; Housley et al., 2009, 1999; Lagostena et al., 2001; Lagostena and Mammano, 2001; Matsunobu and Schacht, 2000), while the functional role of TRP and ACh receptors in different supporting cells is largely unexplored.

3.2. ATP evoked reversible and repeatable Ca^{2+} transients in Deiters' cell soma and process, Hensen's and Caudius cells

Perfusion of ATP (100 µM, 30 s), acting on both P2X and P2Y receptors (Horváth et al., 2016), evoked reversible and repeatable Ca^{2+} transients in all three supporting cell types (Deiters', Hensen's and Claudius' cells) and the phalangeal processes of Deiters' cells (DCp) loaded by electroporation (Fig. 3). High S/N attained by targeted single-cell electroporation was indispensable to image subcellular compartments. ATP responses in cells loaded with electroporation (fura-2/K^+) had better S/N than ATP responses in bulk loaded cells (fura-2/AM; Fig. 1F). DCp (25 apical, 4 middle, 3 basal turn responses) showed the largest ATP-evoked Ca^{2+}

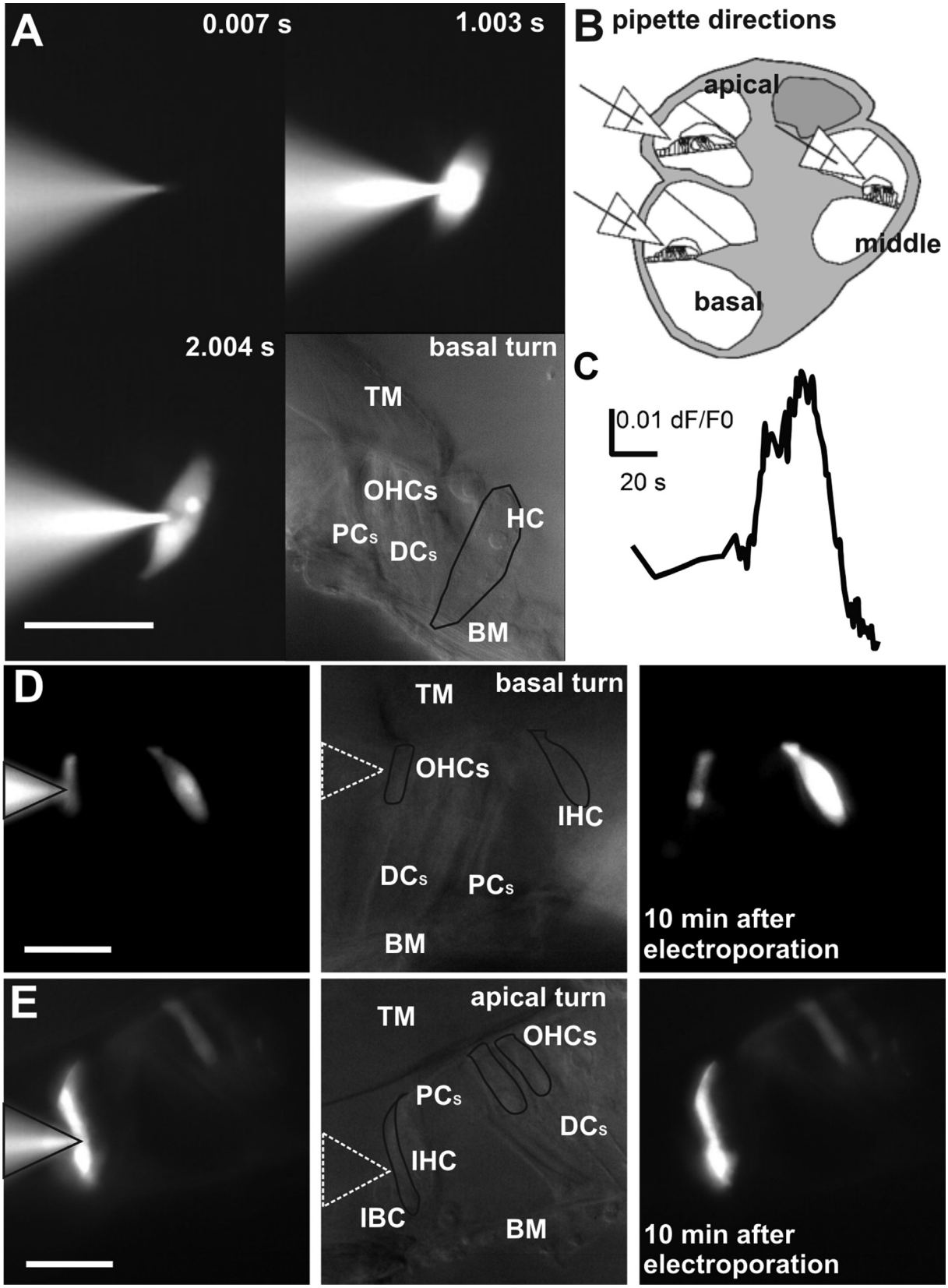

Fig. 2. Procedure of single-cell electroporation. The cells were selected at oblique illumination and approached by glass pipette filled with fluorescent dye (OGB-1, 1 mM). A single square wave current impulse (10 ms, 10 μA) was enough to load the cells within seconds. (A) Course of dye loading by electroporation. Hensen's cell from the basal turn of the mouse cochlea. (B) Schematic drawing of pipette and preparation arrangement. The same pipette orientation was used in all three cochlear turns. (C) ATP evoked Ca^{2+} transient in an inner hair cell. (D) Loading of inner and outer hair cells in the basal turn of a preparation. Left image, moment of electroporation; middle image, oblique illuminated image and location of the pipette; right image, loaded cells 10 min after electroporation. (E) Loading of an inner boarder and an outer hair cell in the apical turn (same sequence of images as in panel D). (OHCs, outer hair cells; DCs, Deiters' cells; PCs, pillar cells; IBC, inner border cell; IHC, inner hair cell; HC, Hensen's cell; BM, basal membrane; TM, tectorial membrane).

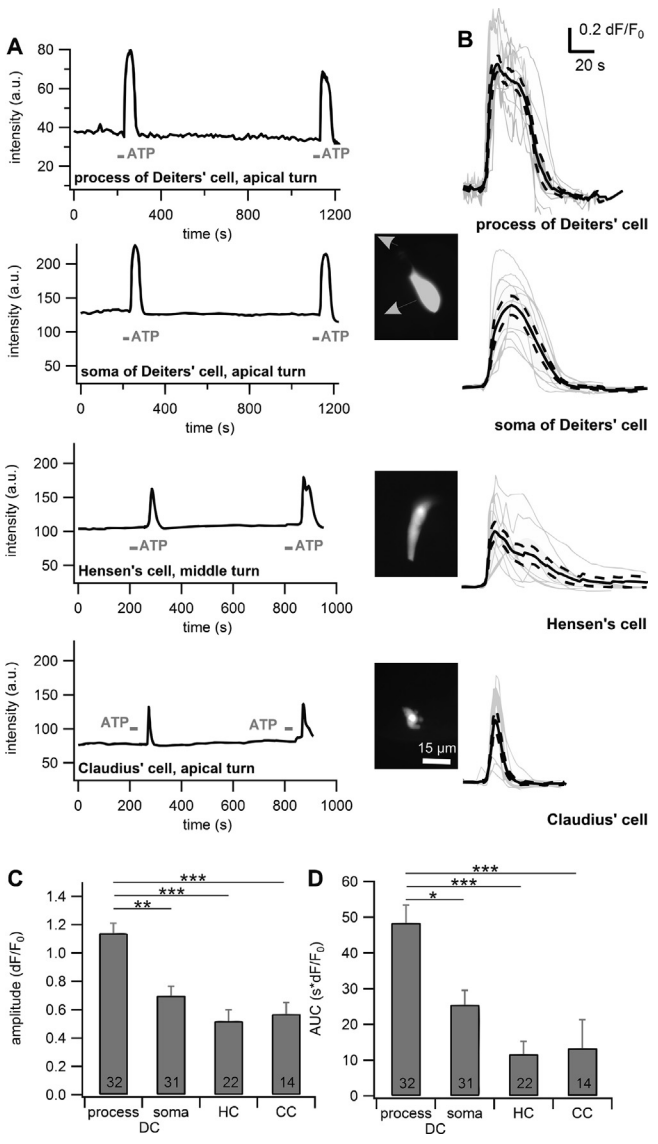

Fig. 3. ATP evoked repeatable Ca^{2+} transients in different supporting cells (Deiters', Hensen's and Claudius') loaded with OGB-1 by electroporation. Perfusion of ATP (100 µM, 30 s), agonist of purinergic receptors, caused the elevation of fluorescent intensity in all types of supporting cells electroporated by the Ca^{2+} sensitive dye OGB-1. The good S/N enabled subcellular imaging in the Deiters' cells. The ATP responses were reversible and repeatable (A) in all three cell types. Averages of 10 responses (dF/F_0, average ± SEM) showed different response kinetics (B). The phalangeal process of Deiters' cells showed the largest Ca^{2+} response in dF/F_0, while the transient amplitudes in the somas of the three supporting cell types did not differ significantly (B, C). Responses of Hensen's cells often had two peaks (A, B). Claudius' cells had a rapidly increasing and decaying response (A, B). Area under the response curve values showed similar relations to each other as the amplitudes (D). Example experiments of Deiters' and Claudius' cells were from the apical and of Hensen's cells from the middle cochlear turn. Number of cells challenged with ATP are given in the respective bars. * $p < 0.05$; ** $p < 0.01$; *** $p < 0.001$.

transient expressed in relative amplitude (dF/F_0; Fig. 3B and C) and response integral (area under the curve, AUC, $s*dF/F_0$; Fig. 3B, D). The amplitudes and AUCs of ATP-evoked Ca^{2+} transients were not significantly different from each other in Deiters' (24 apical, 4 middle, 3 basal turn responses), Hensen's (10 apical, 12 middle, 2 basal turn responses) and Claudius' cell (6 apical, 5 middle, 3 basal turn responses) somas (p-values of the amplitudes: CC-DC: 1; CC-HC: 1; DC-HC: 0.4511; DCp-DC: 0.0018; DCp-HC: $1.47*10^{-6}$; DCp-CC: $2.85*10^{-4}$; p-values of the AUCs: CC-DC: 0.0919; CC-HC: 1; DC-HC: 0.1412; DCp-DC: 0.0163; DCp-HC: $2.46*10^{-6}$; DCp-CC: $1.01*10^{-5}$; Bonferroni post-hoc test; Fig. 3C and D). The shape of Hensen's cells transients was two-peaked in several cases modifying the average response trace. Ca^{2+} transients in Claudius' cells had the fastest decay (Fig. 3B).

Omission of Ca^{2+} from the perfusion buffer decreased the ATP-evoked Ca^{2+} transients in all three supporting cell types, and the Deiters' cell process, although the inhibition was statistically not significant in the Hensen's and Claudius' cells. Readministration of Ca^{2+} resulted in the recovery of the ATP response (Fig. 4) indicating the viability of the cells in the hemicochlea during the whole experiment. Cells not responding to the third ATP stimulus were removed from the analysis.

Inner hair cells could also be stimulated by ATP, although the transients were smaller (Fig. 2C).

3.3. Stimulation of TRPA1 and TRPV1 channels did not induce Ca^{2+} signaling (except AITC in a single Hensen's cell), but TRPA1 activation resulted in the slight movement of the tissue

Anatomical studies (Ishibashi et al., 2008; Velez-Ortega, 2014; Zheng et al., 2003) indicated the presence of TRPA1 and TRPV1 non-selective cation channel receptors on supporting cells of the organ of Corti. In this study, the possible functional role of TRPA1 channels in Ca^{2+} signaling in Deiters', Hensen's and Claudius' cells was tested by the perfusion (30 s) of its agonist, AITC (Sághy et al., 2018, 2015). Before and after AITC the cells were challenged with ATP (100 µM) to demonstrate the viability and responsiveness of the cells during the whole experiment (Fig. 5B and C). Cells not responding to any of these stimulations were excluded from the analysis.

AITC, tested in 200 µM, 400 µM and 2 mM concentrations did not evoke any Ca^{2+} transients, but caused a faint fluctuation of the baseline in a dose-dependent manner (Fig. 5A). Since we visually observed that the cells in the images moved out from and into the focal plane after AITC application, we electroporated the supporting cells with the double excitation Ca^{2+} indicator, fura-2/K^+. The ratio of fluorescence at 340 and 380 nm (F_{340}/F_{380}) is independent of the focal position and geometrical factors (Grynkiewicz et al., 1985) thus it is free of the movement artifacts present on the 340 and 380 nm excitation traces induced by the 400 µM and 2 mM AITC perfusion (Fig. 5B and B inset). By using fura-2/K^+ in the ratiometric mode, we found no Ca^{2+} response for TRPA1 stimulation by AITC either in Deiters' or Claudius' cells. However, the agonist evoked transients with smaller amplitude in one Hensen's cell (P15) out of 7 (~14% response rate; Fig. 5C). The transients of this cell showed a ~40 s slower onset. Subcellular imaging in Deiters' cells was also feasible with fura-2/K^+ (Fig. 5C). The amplitude of the second ATP stimuli were similar to the first ones except in Claudius' cells which showed a decline in the second ATP response after AITC application ($p = 0.008498$).

Capsaicin (330 and 990 nM), the agonist of TRPV1 channels (Sághy et al., 2018, 2015) did not induce any Ca^{2+} response in the supporting cells (Fig. 6). The experimental arrangement (Fig. 6A) was similar to the one testing TRPA1 function. ATP (100 µM) was used to confirm cell viability. Capsaicin administration, unlike AITC, was not followed by any movement in the preparation. The ATP responses recovered after capsaicin in every cell type, even in the Claudius' cells ($p = 0.2413$).

3.4. Activation of ACh receptors by carbachol induced Ca^{2+} response in Deiters' and Hensen's cells

In order to further demonstrate the applicability of targeted electroporation in hemicochlea preparation we applied carbachol, the agonist of ACh receptors. Deiters' and Hensen's cells receive

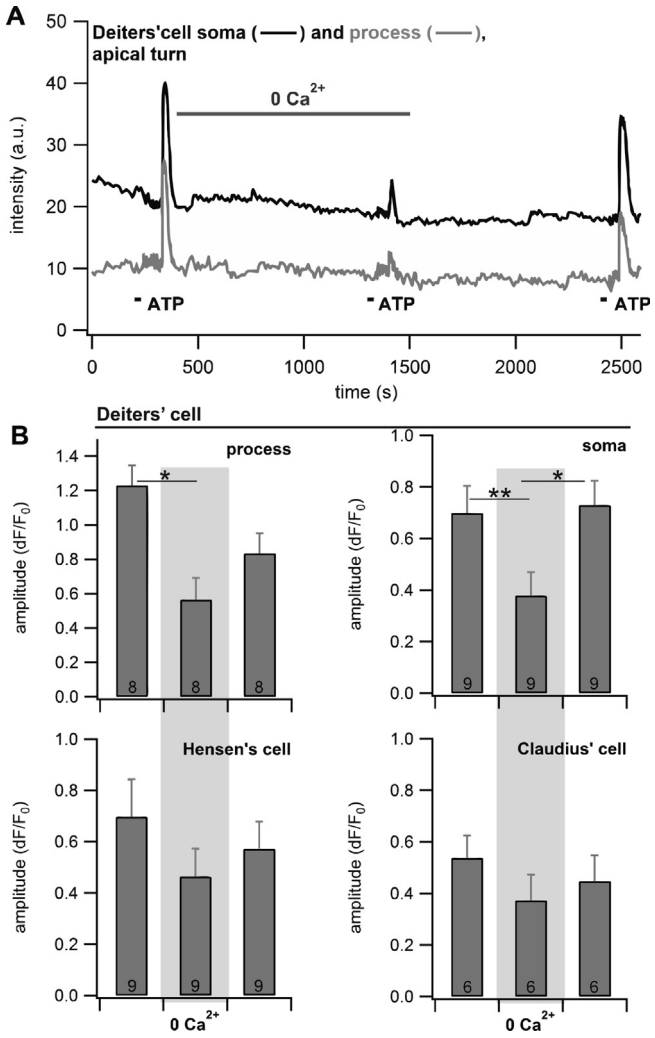

Fig. 4. The model system is suitable for testing the effect of pharmacological manipulations on evoked Ca^{2+} transients - omission of Ca^{2+} inhibited the ATP response. The viability of cells loaded by single-cell electroporation in the hemicochlea preparation allows functional imaging of triple stimulation, thus making the model feasible for comparing the effect of pharmacological manipulations (2nd stimulus) to an internal control (1st stimulus). The recovery of the response to the 3rd stimulation in the absence of the pharmacological intervention validates the result and confirms the preparation viability. Cells without a response to the 3rd stimulus were excluded from the analysis. (A) Subcellular imaging of the effect of Ca^{2+} withdrawal on ATP stimulation in the process and soma of an apical Deiters' cell. (B) The absence of extracellular Ca^{2+} decreased the ATP response in all three cell types loaded with OGB-1, including the process of the Deiters' cells. Number of experiments are given in the respective bars. * $p < 0.05$; ** $p < 0.01$.

efferent innervation, including cholinergic input (Bruce et al., 2000; Burgess et al., 1997; Fechner et al., 2001; Nadol and Burgess, 1994; Raphael and Altschuler, 2003) and evidence supports the presence of the highly Ca^{2+} permeable functional α9 subunit-containing nicotinic ACh receptors (nAChRs) in Deiters' cells isolated from adult guinea-pigs (Matsunobu et al., 2001). Functional role of ACh receptors on Hensen's cells has not been investigated so far.

Carbachol was perfused in 100 μM concentration (30 s). Both compartments of the Deiters' cells were activated by carbachol in 33% of the experiments (Fig. 7A). The amplitudes of these responses were similar to the ATP-induced ones (Fig. 7A and B), but their duration was significantly shorter in the process (ATP: 41.34 ± 5.94 s, carbachol: 17.87 ± 3.43 s, p-value = 0.01667).

One Hensen's cell (in the middle turn of the cochlea) out of 5 was activated by carbachol at 100 μM (Fig. 7C). The response was small, but clearly visible both in its amplitude and AUC. It had only one peak in contrast to a typical ATP induced response in Hensen's cells (Fig. 3).

Viability of the cells was confirmed by ATP application again. Cells not responding to ATP were excluded from the study.

4. Discussion

4.1. Advantages of the mature hemicochlea preparation and drawbacks of bulk loadings in Ca^{2+} imaging

Although the hemicochlea (Edge et al., 1998; Richter et al., 1998) lacks the normal hydrodynamic properties and amplification of the cochlea, the preparation provides several advantages for investigations: i) it sustains the delicate cytoarchitecture of the organ of Corti, ii) allows tonotopic experimental approach on the radial perspective of the organ in the basal, middle and apical turns, and iii) provides all of these in a preparation from hearing mice (>P15; Ehret, 1976). Cell cultures of certain cochlear cell types or acutely isolated cells (Ashmore and Ohmori, 1990; Dulon et al., 1993) do not preserve the special microenvironment and intercellular communication in the organ of Corti. Cochlear explants lack some of these disadvantages, but in their case a restricted portion of the organ of Corti is excised from its environment (Chan and Rouse, 2016; Moser and Beutner, 2000). The explants are usually prepared from neonatal pre-hearing murines (Landegger et al., 2017; Piazza et al., 2007), similarly to the cochlear slices (Lin et al., 2003; Morton-Jones et al., 2008; Ruel et al., 2008). Dissected temporal bone preparation from the guinea-pig provides access only to the apical coil (Fridberger et al., 1998; Mammano et al., 1999). Thus in many characteristics the hemicochlea preparation is superior for physiological investigations in the mature cochlea, identification of the pathomechanisms leading to sensorineural hearing losses (SNHLs) in the adults or deciphering potential drug targets for SNHLs (Lendvai et al., 2011) and testing candidate therapeutic compounds acting on these targets. The preparation was first used by our group for real functional imaging of intracellular Ca^{2+} signaling, which is implicated in the aforementioned phenomena (Horváth et al., 2016). In that study, the indicator dye was bulk loaded in its AM form, as in the majority of Ca^{2+} imaging studies on cells in the cochlea (Chan and Rouse, 2016; Dulon et al., 1993; Matsunobu and Schacht, 2000; Piazza et al., 2007). Bulk loading is convenient, but the dye remains in the extracellular space resulting in significant background staining and low S/N. AM dyes can be taken up by every cell, contaminating the responses of the cell of interest by fluorescence from adjacent responding cells (Fridberger et al., 1998). Furthermore, loading and deesterification take longer time compromising the survival of the preparation. Here, we show the novel method and validation of targeted single-cell electroporation of identified supporting cells in the hemicochlea preparation of the adult mouse cochlea. The improved technique is rapid, reliable and has a significantly better S/N, which enables functional imaging of single cells in the hemicochlea preparation with higher spatial resolution.

4.2. Single-cell electroporation – rapid and specific Ca^{2+} indicator loading of supporting cells with low S/N and retained viability

Single-cell electroporation allows dye loading of selected cells. It has been successfully used in brain slices to load neurons and measure Ca^{2+} signals even in fine structures as dendritic spines (Nevian and Helmchen, 2007). Previously Lin and coworkers (Lin et al., 2003) have reported the targeted electroporation of a spiral ganglion cell, an outer hair cell and an epithelial cell in the

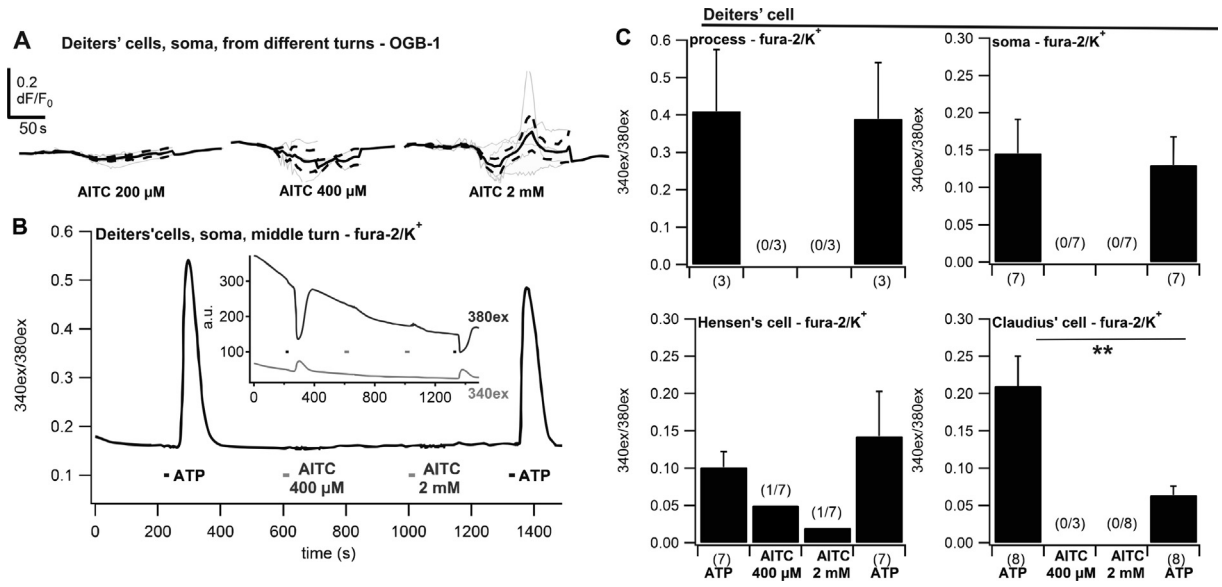

Fig. 5. TRPA1 agonist AITC did not induce $[Ca^{2+}]_i$ changes in the supporting cells of the organ of Corti (except in a single Hensen's cell), but evoked a faint movement of the tissue. (A) Cells loaded with OGB-1 and stimulated by different concentrations of AITC (200 µM, 400 µM and 2 mM; 30 s perfusion) moved out from the focal plane of imaging, but did not respond with measurable $[Ca^{2+}]_i$ changes. See dose-dependent fluctuations of fluorescence on individual and average curves of Deiters' cell soma. (B) Ratiometric imaging after successful loading of fura-2/K^+ by targeted electroporation. Ratiometric measurement eliminated the moving artifact visible on the individual 340 nm and 380 nm excitation curves (*inset*) of a representative experiment. ATP (100 µM) responses at the beginning and at the end of the experiments prove that the lack of AITC (400 µM and 2 mM) effect is not because of lost cellular viability. Cells not responding to ATP were excluded from further analysis. (C) AITC (400 µM and 2 mM) did not induce Ca^{2+} transients in the investigated supporting cell types, except the reduced amplitude transients in a single Hensen's cell (P15) out of the seven. Bars represent change in F_{340}/F_{380} ratio relative to the baseline (dF_{340}/F_{380}). Number of responding/imaged cells is in parentheses. The amplitude of the Ca^{2+} increase is calculated from the responding cells only. ** $p < 0.01$.

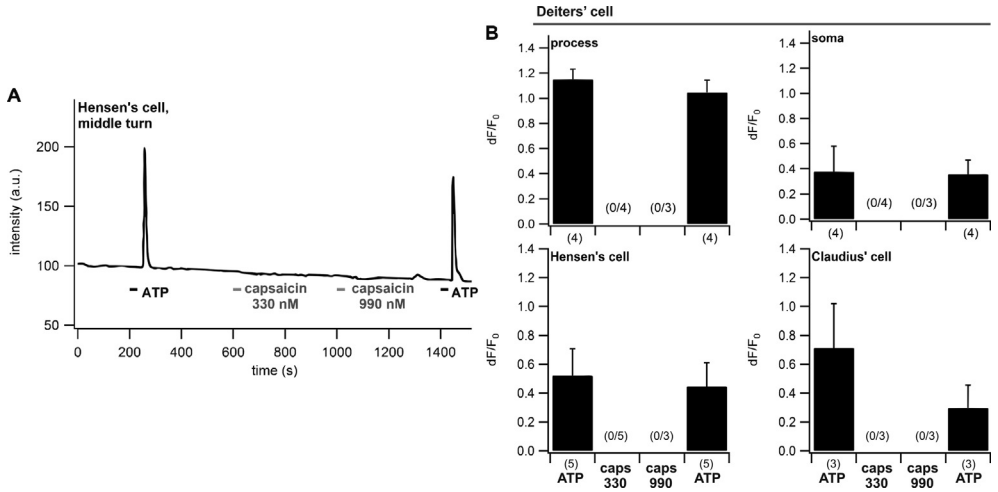

Fig. 6. TRPV1 agonist capsaicin did not induce $[Ca^{2+}]_i$ changes in any of the supporting cell types investigated. (A) Representative trace shows the experimental arrangement. Capsaicin was perfused (30 s) in the concentration of 330 and 990 nM. ATP (100 µM), administered at the beginning and the end of the experiments to prove the viability and responsiveness of the cells. Not responding cells were excluded. (B) Bar graphs show the averages of evoked transients. Capsaicin induced Ca^{2+} response in neither of the cell types (Deiters', Hensen's and Claudius') loaded with OGB-1. Number of responding/imaged cells is in parentheses.

Reissner's membrane, but their actual experiment was performed on cochlear slices from P0-P7 rats and the technique has never been used in follow-up studies. Our success rate of Ca^{2+} indicator loading by electroporation into identified supporting cells in the hemicochlea was similarly high as in the brain slices and the successfully loaded cells nearly all survived. The quick approach of the selected cell and the lack of pressure on the pipette minimized the spillover of the indicator from the pipette. The negligible amount of extracellular fluorescent dye and the specific cell loading enabled subcellular functional imaging of the soma and the process of Deiters' cells, i.e. the stalk and the phalangeal process of the Deiters' cells were not obscured by the fluorescence of outer hair cells. Ca^{2+} imaging in Deiters' cells at the subcellular level has only been performed before in isolated cells (Dulon et al., 1993) or with simultaneous whole-cell patch-clamp recording (Lagostena and Mammano, 2001), which is a laborious technique and washes out the intracellular biomolecules involved in signaling (Ishikawa et al., 2002; Vyleta and Jonas, 2014). Electroporation is suitable for loading more cells in a preparation. We have also managed to do that in the hemicochlea preparation (Fig. 2). However, electroporation and bulk loading are not mutually exclusive. The latter one is favorable if loading of high number of cells is required, e.g. for

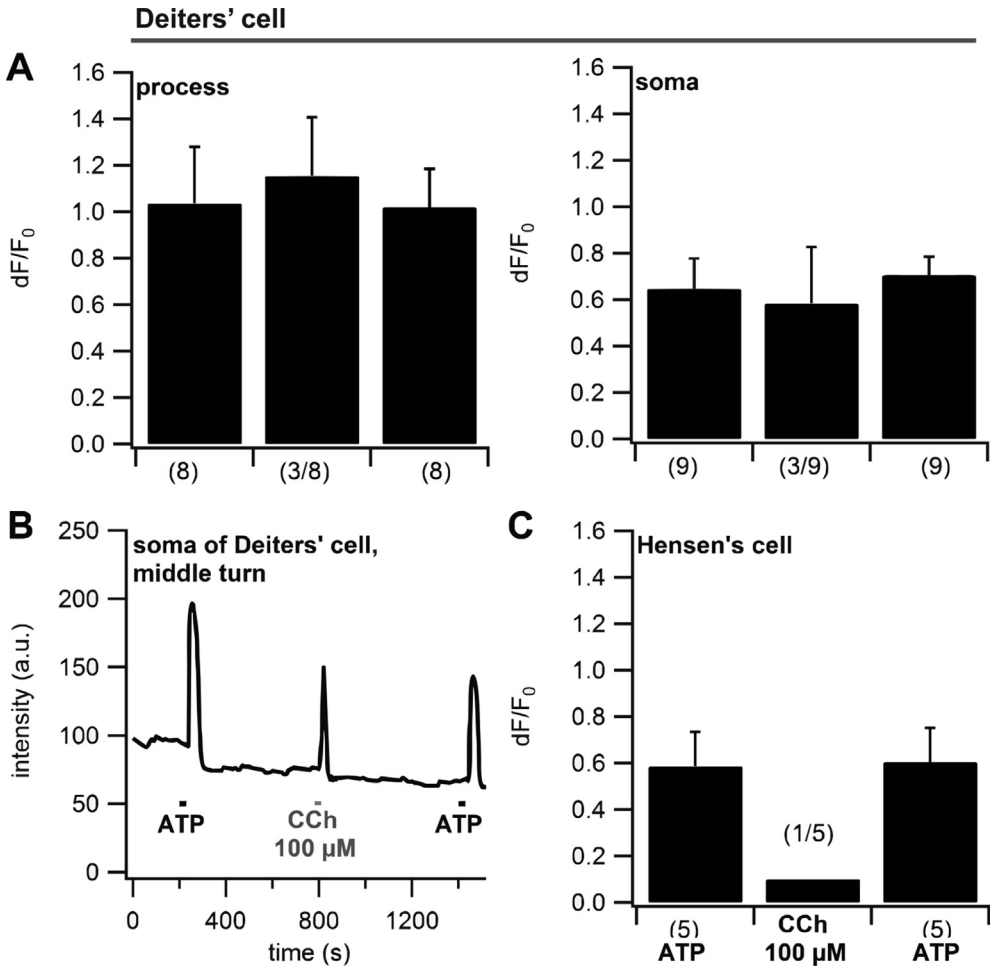

Fig. 7. Carbachol, a cholinergic receptor agonist, induced $[Ca^{2+}]_i$ transients in Deiters' and Hensen's cells. (A) Deiters' cells loaded with OGB-1 were activated by the perfusion of carbachol (100 µM, 30 s perfusion) in 33% of the experiments. (B) A representative carbachol-evoked response in a middle-turn Deiters' cell. The amplitude of the transient was comparable to the ATP induced responses, however, its duration was shorter. (C) We detected intensity elevation in one out of five Hensen's cells (20%) after the carbachol stimulus. The amplitude of the Ca^{2+} increase is calculated from the responding cells only. Number of responding/imaged cells is in parentheses.

investigating Ca^{2+} waves travelling through a larger population of supporting cells in the cochlea. On the other hand, if spatial resolution and a radial view of the adult organ of Corti is important for a given cochlear study, targeted single-cell electroporation in the hemicochlea preparation is a simple, rapid and reliable choice.

The electroporation worked well for the Deiters', Hensen's and Claudius' cells. In contrast, the pillar cells could not be loaded homogenously, because the dye did not diffuse through the stalk part of the cell. We have not experienced any problem of dye diffusion through the stalk of the Deiters' cells. Dye compartmentalization in this cell type only appeared when the glass pipette was mistargeted, pushed deep inside the cell and reached the microtubule bundle directly. This happened rarely with an experienced experimenter and became easily recognizable by the visible bundles (Supplementary Fig 1.). Inner and outer hair cells could also be loaded successfully.

4.3. ATP evoked Ca^{2+} transients in the soma of Deiters', Hensen's and Claudius' cells and the phalangeal process of the Deiters' cells - validation of (sub)cellular imaging

Viability of the loaded cells and applicability of the method for functional imaging of intracellular Ca^{2+} signaling were tested by measuring the ATP-evoked responses. ATP is a ubiquitous transmitter in the hearing organ and its role in purinergic receptor-mediated Ca^{2+} signaling is well substantiated (Housley et al., 2009; Lee and Marcus, 2008; Mammano et al., 2007). Previously, we have also demonstrated its effect in Deiters', Hensen's and pillar cells in the hemicochlea preparation after bulk loading with fura-2/AM (Horváth et al., 2016). ATP induced reversible and repeatable Ca^{2+} transients in all three electroporation loaded supporting cell types with higher S/N compared to bulk loading. In Deiters' cells, which have two well defined compartments the selective loading and the low background fluorescence allowed us to perform subcellular imaging, thus we could measure ATP- and carbachol-evoked Ca^{2+} transients in the soma and the plate of the phalangeal process. The ATP responses had somewhat different characteristics in different supporting cells. The Hensen' cells frequently had two-peak Ca^{2+} responses while the Claudius' cells showed the fastest recovery after stimulation.

The processes of Deiters' cells had the largest Ca^{2+} transients, expressed in dF/F_0, probably because of the largest density of ATP receptors on their surface. However, the lower baseline fluorescence (F_0), or the tiny volume of the process with larger surface-to-volume ratios may further contribute to the difference by promoting the Ca^{2+} accumulation compared to the somas with smaller surface-to-volume ratios (Helmchen et al., 1997). Quantification of basal Ca^{2+} concentration and its changes in absolute concentration

values requires dual wavelength indicators or dual indicators loading and calibration (Yasuda et al., 2004). Nevertheless, our hemicochlea electroporation method provides a reliable tool to investigate the supporting cell Ca^{2+} signaling at the single cell and subcellular level in more details.

Functional expression of both ionotropic P2X and metabotropic P2Y receptors of ATP have been shown on supporting cells in the organ of Corti in neonatal rodents and hearing mice (P15-21) (Horváth et al., 2016; Housley et al., 2009; Lee and Marcus, 2008). Partial inhibition of the ATP transients by omission of Ca^{2+} from the perfusion buffer, a blunt way of separating the extracellular Ca^{2+}-dependent P2X- and intracellular store-dependent P2Y receptor responses reproduced the results in the literature and further validated the method. Furthermore, this arrangement of the experiment, when Ca^{2+} transients are evoked in the absence then in the presence of Ca^{2+} in the same cell, demonstrated the way how pharmacological interventions can be tested by internal control and provide a lower variability of the effects. The development of the 3rd stimulus in the absence of the pharmacological inhibitor or modulator can confirm the viability of the cell and the effect of the tested drug.

Unraveling the causes of the smaller amplitudes of ATP-evoked transients, we measured in inner hair cells would require more extensive examination.

4.4. TRPA1 stimulation did not induce Ca^{2+} response in Deiters' and Claudius' cells but raised the possibility of TRPA1 role in Hensen's cell Ca^{2+} homeostasis

TRP channels have mostly been studied by anatomical methods and their presence has been shown in the inner ear. We tested the effect of the TRPA1 agonist AITC and the TRPV1 agonist capsaicin on Ca^{2+} regulation in the supporting cells of the mouse organ of Corti. TRPA1 channels have been shown in the supporting cells, mostly in Hensen's cells (Corey et al., 2004; Stepanyan et al., 2011; Velez-Ortega, 2014), but also in Deiters', Claudius' and pillar cells (Velez-Ortega, 2014). In newborn rodent cochlear explant the TRPA1 antibodies seem to be nonspecific or appear in the endoplasmic reticulum in Hensen's and Claudius' cells (Corey et al., 2004). However, indirect immunolabeling (against TRPA1 promoter connected reporter gene) confirmed TRPA1 presence in the neonatal cochlear explants (Velez-Ortega, 2014). Contrarily, Takumida et al. (2009) reported immunoreactivity to TRPA1 channels exclusively in nerve fibers of the spiral ganglion cells and in nerves innervating the outer or inner hair cells in the mouse inner ear. We could not detect Ca^{2+} response at any AITC concentrations in the investigated supporting cells, except reduced-amplitude and late-onset transients in a single Hensen's cell.

The decrease in the amplitudes of ATP transients after AITC applications in Claudius' cells may be the consequence of a functional cross-inhibition between co-expressed TRPA1 and the purinergic P2X receptors in that cells (Stanchev et al., 2009). Note that in the absence of these insults the ATP response recovered (Fig. 3).

4.5. TRPA1 stimulation displaced the organ of Corti

On the other hand, we detected a dose-dependent movement 'artifact' in the images after AITC application. This probably represents a displacement of the whole organ of Corti (and not intracellular Ca^{2+} concentration changes) and could be caused by AITC-evoked contraction of cells in the cochlear epithelium. Outer hair cells may be involved in this contraction (Corey et al., 2004). However, Velez-Ortega (2014) suggested the contraction of pillar and Deiters' cells as the origin of TRPA1 stimulation-evoked tissue movement in P0-P7 wild type mice. The contraction was not induced in Trpa1−/− mice. Our study is in contrast to the idea of TRPA1-evoked contraction of mature Deiters' cells or, alternatively, it is not exerted by intracellular Ca^{2+} increase. Use of TRPA1 KO mice could contribute to decipher the role of TRPA1 channels.

4.6. TRPV1 stimulation did not evoke any Ca^{2+} response in the supporting cells

The presence of TRPV1 channels has also been shown in the cochlear epithelium. Their expression was dependent on rodent species and age. In mouse cochlea the TRPV1 RNA level first increased then declined in the E18-P8 period, similarly to TRPA1 (Asai et al., 2009). On the contrary, Scheffer at al (Scheffer et al., 2015) did not detect RNA for TRPV1 in hair cells and surrounding cells in E16-P7 mice. Immunohistochemistry was used in adult guinea-pigs and rats to show the presence of TRPV1 in some supporting cells, particularly in Hensen's and outer and inner pillar cells (Takumida et al., 2005; Zheng et al., 2003). The lack of capsaicin response in our experiments may indicate the absence of TRPV1 channels in Deiters', Hensen's or Claudius' cells in the P15-21 mouse cochlea. Indeed they have not been directly demonstrated on these cell types yet. Alternatively, they are functionally not involved in intracellular Ca^{2+} regulation in these cells. We did not observe any movement in response to capsaicin in the preparation either, suggesting that TRPV1 is not involved in contraction of cells in the organ of Corti in hearing mice.

4.7. ACh receptor activation evoked Ca^{2+} transients in some Deiters' and Hensen's cells

Cholinergic efferent innervation of the motile outer hair cells has a well-known role in setting cochlear amplification (Dallos et al., 1997; Kujawa et al., 1994). Deiters' and Hensen's cells also receive efferent innervation (Bruce et al., 2000; Burgess et al., 1997; Fechner et al., 2001; Nadol and Burgess, 1994; Raphael and Altschuler, 2003). Matsunobu and his coworkers have shown acetylcholine-evoked Ca^{2+} increase in isolated Deiters' cells from guinea-pigs and suggested the involvement of α9-subunit containing nAChRs (Matsunobu et al., 2001). The presence of α10-subunit of nAChRs was not ruled out either in adult rat Deiters' cells (Elgoyhen et al., 2001). Both homomeric α9 and heteromeric α9α10 nAChRs are highly permeable for Ca^{2+} what can be detected by Ca^{2+} imaging methods (Fucile et al., 2006; Matsunobu et al., 2001). There are no similar receptor expression or functional data on Hensen's cells in the literature, thus we investigated the effect of carbachol, a partial agonist on both native and α9-subunit containing nAChRs (Verbitsky et al., 2000), also on Hensen's cells. The proportion of Deiters' cells (33%) responding to carbachol was very similar to the one Matsonubu et al. (Matsunobu et al., 2001) reported in isolated guinea-pig Deiters' cells for acetylcholine (42–44%). The response rate of Hensens' cells was only 20% and the amplitude of the Ca^{2+} transient was smaller than that of the ATP-evoked one, differing from Deiters' cells in which carbachol and ATP transients were comparable in amplitude. In addition to confirming the cholinergic responsiveness of Deiters' cells in an *in situ* preparation, we also raised the possibility of cholinergic regulation in Hensens' cells, the other innervated supporting cell type in the organ of Corti.

5. Conclusions

Here we presented the method of Ca^{2+} indicator loading of supporting cells in the organ of Corti in the mature mouse hemicochlea preparation using targeted single-cell electroporation. Ca^{2+} is an important intracellular messenger and regulator and the

method is a reliable and straightforward tool for elucidating its role in these cells. Indicator loading is always a crucial step in functional imaging. Our method provides several advantages: i.) it is possible to perform in the adult hearing cochlea, ii.) rapid, thus extends the experimental time window, iii.) selective, therefore lowers S/N and allows subcellular imaging, iv.) free from washing out the intracellular biomolecules involved in signaling and metabolism and v.) suitable for tonotopic investigations on the radial perspective in the basal, middle and apical turns of the cochlea.

Confirming the effect of ATP in Deiters', Hensen's and Claudius' cells and supporting the functional role of AChRs in Deiters' and Hensen's cells in an *in situ* preparation also served as a validation of the method. Showing the lack of involvement of TRPA1 and TRPV1 channels in Ca^{2+} regulation in Deiters' and Claudius' cells and in Deiters', Hensen's and Claudius' cells, respectively, and raising the possibility of the functional role of ACh and TRPA1 channels in Hensen's cell Ca^{2+} homeostasis demonstrated the applicability of the method in the exploration of new Ca^{2+} signaling pathways in supporting cells of the mature cochlea.

Acknowledgments

This work was supported by the Higher Education Institutional Excellence Programme of the Ministry of Human Capacities in Hungary, within the framework of the Neurology thematic programme of the Semmelweis University (FIKP 2018), the Hungarian Scientific Research Fund (NKFI K 128875) and the Hungarian-French Collaborative R&I Programme on Biotechnologies (TÉT_10-1-2011-0421). We thank Peter Dallos and Claus-Peter Richter for teaching us the preparation of the hemicochlea.

Appendix A. Supplementary data

Supplementary data to this article can be found online at https://doi.org/10.1016/j.heares.2018.11.004.

References

Asai, Y., Holt, J.R., Géléoc, G.S.G., 2009. A quantitative analysis of the spatiotemporal pattern of transient receptor potential gene expression in the developing mouse cochlea. J. Assoc. Res. Otolaryngol. 11, 27–37. https://doi.org/10.1007/s10162-009-0193-8.

Ashmore, J.F., Ohmori, H., 1990. Control of intracellular calcium by ATP in isolated outer hair cells of the Guinea-pig cochlea. J. Physiol. 428, 109–131.

Berridge, M.J., 2016. The inositol trisphosphate/calcium signaling pathway in health and disease. Physiol. Rev. 96, 1261–1296. https://doi.org/10.1152/physrev.00006.2016.

Beurg, M., Fettiplace, R., Nam, J.-H., Ricci, A.J., 2009. Localization of inner hair cell mechanotransducer channels using high-speed calcium imaging. Nat. Neurosci. 12, 553–558. https://doi.org/10.1038/nn.2295.

Bruce, L.L., Christensen, M.A., Warr, W.B., 2000. Postnatal development of efferent synapses in the rat cochlea. J. Comp. Neurol. 423, 532–548.

Burgess, B.J., Adams, J.C., Nadol, J.B., 1997. Morphologic evidence for innervation of Deiters' and Hensen's cells in the Guinea pig. Hear. Res. 108, 74–82.

Chan, D.K., Rouse, S.L., 2016. Sound-induced intracellular Ca2+ dynamics in the adult hearing cochlea. PLoS One 11, e0167850. https://doi.org/10.1371/journal.pone.0167850.

Corey, D.P., García-Añoveros, J., Holt, J.R., Kwan, K.Y., Lin, S.-Y., Vollrath, M. a, Amalfitano, A., Cheung, E.L.-M., Derfler, B.H., Duggan, A., Géléoc, G.S.G., Gray, P. a, Hoffman, M.P., Rehm, H.L., Tamasauskas, D., Zhang, D.-S., 2004. TRPA1 is a candidate for the mechanosensitive transduction channel of vertebrate hair cells. Nature 432, 723–730. https://doi.org/10.1038/nature03066.

Dallos, P., He, D.Z., Lin, X., Sziklai, I., Mehta, S., Evans, B.N., 1997. Acetylcholine, outer hair cell electromotility, and the cochlear amplifier. J. Neurosci. 17, 2212–2226.

Denk, W., Holt, J.R., Shepherd, G.M.G., Coreytt, D.P., 1995. Calcium imaging of single stereocilia in hair cells: localization of transduction channels at both ends of tip links. Neuron. https://doi.org/10.1016/0896-6273(95)90010-1.

Dulon, D., Moataz, R., Mollard, P., 1993. Characterization of Ca2+ signals generated by extracellular nucleotides in supporting cells of the organ of Corti. Cell Calcium 14, 245–254.

Edge, R.M., Evans, B.N., Pearce, M., Richter, C., Hu, X., Dallos, P.Y., 1998. Morphology of the unfixed cochlea. Hear. Res. 124, 1–16.

Ehret, G., 1976. Development of absolute auditory thresholds in the house mouse (Mus musculus). J. Am. Audiol. Soc. 1, 179–184.

Elgoyhen, A.B., Vetter, D.E., Katz, E., Rothlin, C.V., Heinemann, S.F., Boulter, J., 2001. alpha10: a determinant of nicotinic cholinergic receptor function in mammalian vestibular and cochlear mechanosensory hair cells. Proc. Natl. Acad. Sci. U. S. A 98, 3501–3506. https://doi.org/10.1073/pnas.051622798.

Emadi, G., 2003. Stiffness of the gerbil basilar membrane: radial and longitudinal variations. J. Neurophysiol. 91, 474–488. https://doi.org/10.1152/jn.00446.2003.

Fechner, F.P., Nadol JB, J.R., Burgess, B.J., Brown, M.C., 2001. Innervation of supporting cells in the apical turns of the Guinea pig cochlea is from type II afferent fibers. J. Comp. Neurol. 429, 289–298.

Fettiplace, R., Kim, K.X., 2014. The physiology of mechanoelectrical transduction channels in hearing. Physiol. Rev. 94, 951–986. https://doi.org/10.1152/physrev.00038.2013.

Fridberger, A., Flock, A., Ulfendahl, M., Flock, B., 1998. Acoustic overstimulation increases outer hair cell Ca2+ concentrations and causes dynamic contractions of the hearing organ. Proc. Natl. Acad. Sci. U. S. A 95, 7127–7132.

Fucile, S., Sucapane, A., Eusebi, F., 2006. Ca2+ permeability through rat cloned α9-containing nicotinic acetylcholine receptors. Cell Calcium 39, 349–355. https://doi.org/10.1016/j.ceca.2005.12.002.

Grynkiewicz, G., Poenie, M., Tsien, R.Y., 1985. A new generation of Ca2+ indicators with greatly improved fluorescence properties. J. Biol. Chem. 260, 3440–3450.

He, D.Z.Z., Jia, S., Dallos, P., 2004. Mechanoelectrical transduction of adult outer hair cells studied in a gerbil hemicochlea. Nature 429, 766–770. https://doi.org/10.1038/nature02591.

Helmchen, F., Borst, J.G., Sakmann, B., 1997. Calcium dynamics associated with a single action potential in a CNS presynaptic terminal. Biophys. J. 72, 1458–1471. https://doi.org/10.1016/S0006-3495(97)78792-7.

Horikawa, K., 2015. Recent progress in the development of genetically encoded Ca2+ indicators. J. Med. Invest. 62, 24–28. https://doi.org/10.2152/jmi.62.24.

Horváth, T., Polony, G., Fekete, Aller, M., Halmos, G., Lendvai, B., Heinrich, A., Sperlágh, B., Vizi, E.S., Zelles, T., 2016. ATP-evoked intracellular Ca2+ signaling of different supporting cells in the hearing mouse hemicochlea. Neurochem. Res. 41, 364–375. https://doi.org/10.1007/s11064-015-1818-4.

Housley, G.D., Bringmann, A., Reichenbach, A., 2009. Purinergic signaling in special senses. Trends Neurosci. 32, 128–141. https://doi.org/10.1016/j.tins.2009.01.001.

Housley, G.D., Kanjhan, R., Raybould, N.P., Greenwood, D., Salih, S.G., Järlebark, L., Burton, L.D., Setz, V.C., Cannell, M.B., Soeller, C., Christie, D.L., Usami, S., Matsubara, A., Yoshie, H., Ryan, A.F., Thorne, P.R., 1999. Expression of the P2X(2) receptor subunit of the ATP-gated ion channel in the cochlea: implications for sound transduction and auditory neurotransmission. J. Neurosci. 19, 8377–8388.

Hu, X., Evans, B.N., Dallos, P., 1999. Direct visualization of organ of corti kinematics in a hemicochlea. J. Neurophysiol. 82, 2798–2807. https://doi.org/10.1152/jn.1999.82.5.2798.

Ishibashi, T., Takumida, M., Akagi, N., Hirakawa, K., Anniko, M., 2008. Expression of transient receptor potential vanilloid (TRPV) 1, 2, 3, and 4 in mouse inner ear. Acta Otolaryngol. 128, 1286–1293. https://doi.org/10.1080/00016480801938958.

Ishikawa, T., Sahara, Y., Takahashi, T., 2002. A single packet of transmitter does not saturate postsynaptic glutamate receptors. Neuron 34, 613–621.

Keiler, S., Richter, C.-P., 2001. Cochlear dimensions obtained in hemicochleae of four different strains of mice: CBA/CaJ, 129/CD1, 129/SvEv and C57BL/6J. Hear. Res. 162, 91–104.

Kujawa, S.G., Glattke, T.J., Fallon, M., Bobbin, R.P., 1994. A nicotinic-like receptor mediates suppression of distortion product otoacoustic emissions by contralateral sound. Hear. Res. 74, 122–134.

Lagostena, L., Ashmore, J.F., Kachar, B., Mammano, F., 2001. Purinergic control of intercellular communication between Hensen's cells of the Guinea-pig cochlea. J. Physiol. 531, 693–706.

Lagostena, L., Mammano, F., 2001. Intracellular calcium dynamics and membrane conductance changes evoked by Deiters' cell purinoceptor activation in the organ of Corti. Cell Calcium 29, 191–198. https://doi.org/10.1054/ceca.2000.0183.

Lahne, M., Gale, J.E., 2008. Damage-induced activation of ERK1/2 in cochlear supporting cells is a hair cell death-promoting signal that depends on extracellular ATP and calcium. J. Neurosci. 28, 4918–4928. https://doi.org/10.1523/JNEUROSCI.4914-07.2008.

Landegger, L.D., Dilwali, S., Stankovic, K.M., 2017. Neonatal murine cochlear explant technique as an in vitro screening tool in hearing Research. JoVE e55704–e55704. https://doi.org/10.3791/55704.

Lee, J.H., Marcus, D.C., 2008. Purinergic signaling in the inner ear. Hear. Res. 235, 1–7. https://doi.org/10.1016/j.heares.2007.09.006.

Lelli, A., Asai, Y., Forge, A., Holt, J.R., Geleoc, G.S.G., 2009. Tonotopic gradient in the developmental acquisition of sensory transduction in outer hair cells of the mouse cochlea. J. Neurophysiol. 101, 2961–2973. https://doi.org/10.1152/jn.00136.2009.

Lendvai, B., Halmos, G.B., Polony, G., Kapocsi, J., Horváth, T., Aller, M., Sylvester Vizi, E., Zelles, T., 2011. Chemical neuroprotection in the cochlea: the modulation of dopamine release from lateral olivocochlear efferents. Neurochem. Int. 59, 150–158. https://doi.org/10.1016/j.neuint.2011.05.015.

Lin, X., Webster, P., Li, Q., Chen, S., Ouyang, Y., 2003. Optical recordings of Ca2+ signaling activities from identified inner ear cells in cochlear slices and hemicochleae. Brain Res. Brain Res. Protoc. 11, 92–100.

Lorincz, T., Kisfali, M., Lendvai, B., Sylvester Vizi, E., 2016. Phenotype-dependent Ca2+dynamics in single boutons of various anatomically identified GABAergic

interneurons in the rat hippocampus. Eur. J. Neurosci. 43, 536–547. https://doi.org/10.1111/ejn.13131.
Mammano, F., Bortolozzi, M., Ortolano, S., Anselmi, F., 2007. Ca2+ signaling in the inner ear. Physiology 22, 131–144. https://doi.org/10.220.33.2.
Mammano, F., Frolenkov, G.I., Lagostena, L., Belyantseva, I.A., Kurc, M., Dodane, V., Colavita, A., Kachar, B., 1999. ATP-Induced Ca(2+) release in cochlear outer hair cells: localization of an inositol triphosphate-gated Ca(2+) store to the base of the sensory hair bundle. J. Neurosci. 19, 6918–6929.
Matsunobu, T., Chung, J.W., Schacht, J., 2001. Acetylcholine-evoked calcium increases in Deiters' cells of the Guinea pig cochlea suggest α9-like receptors. J. Neurosci. Res. 63, 252–256. https://doi.org/10.1002/1097-4547(20010201)63:3%3c252::AID-JNR1018%3e3.0.CO;2-0.
Matsunobu, T., Schacht, J., 2000. Nitric oxide/cyclic GMP pathway attenuates ATP-evoked intracellular calcium increase in supporting cells of the Guinea pig cochlea. J. Comp. Neurol. 423, 452–461.
Michalski, N., Michel, V., Caberlotto, E., Lefèvre, G.M., van Aken, A.F.J., Tinevez, J.-Y., Bizard, E., Houbron, C., Weil, D., Hardelin, J.-P., Richardson, G.P., Kros, C.J., Martin, P., Petit, C., 2009. Harmonin-b, an actin-binding scaffold protein, is involved in the adaptation of mechanoelectrical transduction by sensory hair cells. Pflügers Archiv 459, 115–130. https://doi.org/10.1007/s00424-009-0711-x.
Monzack, E.L., Cunningham, L.L., 2013. Lead roles for supporting actors: critical functions of inner ear supporting cells. Hear. Res. https://doi.org/10.1016/j.heares.2013.01.008.
Morton-Jones, R.T., Cannell, M.B., Housley, G.D., 2008. Ca2+ entry via AMPA-type glutamate receptors triggers Ca2+-induced Ca2+ release from ryanodine receptors in rat spiral ganglion neurons. Cell Calcium 43, 356–366. https://doi.org/10.1016/j.ceca.2007.07.003.
Moser, T., Beutner, D., 2000. Kinetics of exocytosis and endocytosis at the cochlear inner hair cell afferent synapse of the mouse. Proc. Natl. Acad. Sci. U. S. A 97, 883–888.
Nadol, J.B., Burgess, B.J., 1994. Supranuclear efferent synapses on outer hair cells and Deiters' cells in the human organ of Corti. Hear. Res. 81, 49–56.
Nevian, T., Helmchen, F., 2007. Calcium indicator loading of neurons using single-cell electroporation. Pflügers Archiv 454, 675–688. https://doi.org/10.1007/s00424-007-0234-2.
Piazza, V., Ciubotaru, C.D., Gale, J.E., Mammano, F., 2007. Purinergic signalling and intercellular Ca2+ wave propagation in the organ of Corti. Cell Calcium 41, 77–86. https://doi.org/10.1016/j.ceca.2006.05.005.
Raphael, Y., Altschuler, R.A., 2003. Structure and innervation of the cochlea. Brain Res. Bull. 60, 397–422. https://doi.org/10.1016/S0361-9230(03)00047-9.
Richter, C.P., Evans, B.N., Edge, R., Dallos, P., 1998. Basilar membrane vibration in the gerbil hemicochlea. J. Neurophysiol. 79, 2255–2264. https://doi.org/10.1152/jn.1998.79.5.2255.
Ruel, J., Chabbert, C., Nouvian, R., Bendris, R., Eybalin, M., Leger, C.L., Bourien, J., Mersel, M., Puel, J.-L., 2008. Salicylate enables cochlear arachidonic-acid-sensitive NMDA receptor responses. J. Neurosci. 28, 7313–7323. https://doi.org/10.1523/JNEUROSCI.5335-07.2008.
Rungta, R.L., Choi, H.B., Tyson, J.R., Malik, A., Dissing-Olesen, L., Lin, P.J.C., Cain, S.M., Cullis, P.R., Snutch, T.P., MacVicar, B.A., 2015. The cellular mechanisms of neuronal swelling underlying cytotoxic edema. Cell 161, 610–621. https://doi.org/10.1016/j.cell.2015.03.029.
Rybak, L.P., Whitworth, C., Scott, V., 1992. Development of endocochlear potential and compound action potential in the rat. Hear. Res. 59, 189–194. https://doi.org/10.1016/0378-5955(92)90115-4.
Sághy, É., Payrits, M., Bíró-Sütő, T., Skoda-Földes, R., Szánti-Pintér, E., Erostyák, J., Makkai, G., Sétáló, G., Kollár, L., Kőszegi, T., Csepregi, R., Szolcsányi, J., Helyes, Z., Szőke, É., 2018. Carboxamido steroids inhibit the opening properties of transient receptor potential ion channels by lipid raft modulation. J. Lipid Res. 59, 1851–1863. https://doi.org/10.1194/jlr.M084723.
Sághy, É., Szőke, É., Payrits, M., Helyes, Z., Börzsei, R., Erostyák, J., Jánosi, T.Z., Sétáló, G., Szolcsányi, J., 2015. Evidence for the role of lipid rafts and sphingomyelin in Ca2+-gating of Transient Receptor Potential channels in trigeminal sensory neurons and peripheral nerve terminals. Pharmacol. Res. 100, 101–116. https://doi.org/10.1016/j.phrs.2015.07.028.
Scheffer, D.I., Shen, J., Corey, D.P., Chen, Z.-Y., 2015. Gene expression by mouse inner ear hair cells during development. J. Neurosci. 35, 6366–6380. https://doi.org/10.1523/JNEUROSCI.5126-14.2015.
Schindelin, J., Arganda-Carreras, I., Frise, E., Kaynig, V., Longair, M., Pietzsch, T., Preibisch, S., Rueden, C., Saalfeld, S., Schmid, B., Tinevez, J.-Y., White, D.J., Hartenstein, V., Eliceiri, K., Tomancak, P., Cardona, A., 2012. Fiji: an open-source platform for biological-image analysis. Nat. Methods 9, 676–682. https://doi.org/10.1038/nmeth.2019.
Stanchev, D., Blosa, M., Milius, D., Gerevich, Z., Rubini, P., Schmalzing, G., Eschrich, K., Schaefer, M., Wirkner, K., Illes, P., 2009. Cross-inhibition between native and recombinant TRPV1 and P2X(3) receptors. Pain 143, 26–36. https://doi.org/10.1016/j.pain.2009.01.006.
Stepanyan, R.S., Indzhykulian, A.A., Vélez-Ortega, A.C., Boger, E.T., Steyger, P.S., Friedman, T.B., Frolenkov, G.I., 2011. TRPA1-mediated accumulation of aminoglycosides in mouse cochlear outer hair cells. J. Assoc. Res. Otolaryngol. 12, 729–740. https://doi.org/10.1007/s10162-011-0288-x.
Takumida, M., Ishibashi, T., Hamamoto, T., Hirakawa, K., Anniko, M., 2009. Expression of transient receptor potential channel melastin (TRPM) 18 and TRPA1 (ankyrin) in mouse inner ear. Acta Otolaryngol. 129, 1050–1060. https://doi.org/10.1080/00016480802570545.
Takumida, M., Kubo, N., Ohtani, M., Suzuka, Y., Anniko, M., 2005. Transient receptor potential channels in the inner ear: presence of transient receptor potential channel subfamily 1 and 4 in the Guinea pig inner ear. Acta Otolaryngol. 125, 929–934. https://doi.org/10.1080/00016480510038572.
Teudt, I.U., Richter, C.P., 2007. The hemicochlea preparation of the Guinea pig and other mammalian cochleae. J. Neurosci. Methods 162, 187–197. https://doi.org/10.1016/j.jneumeth.2007.01.012.
Velez-Ortega, A.C., 2014. Trpa1 Channels in Cochlear Supporting Cells Regulate Hearing Sensitivity after Noise Exposure. University of Kentucky. https://ukno.wledge.uky.edu/physiology_etds/20.
Verbitsky, M., Rothlin, C.V., Katz, E., Belén Elgoyhen, A., 2000. Mixed nicotinic-muscarinic properties of the α9 nicotinic cholinergic receptor. Neuropharmacology 39, 2515–2524. https://doi.org/10.1016/S0028-3908(00)00124-6.
Vyleta, N.P., Jonas, P., 2014. Loose coupling between Ca2+ channels and release sensors at a plastic hippocampal synapse. Science 343, 665–670. https://doi.org/10.1126/science.1244811.
Yasuda, R., Nimchinsky, E.A., Scheuss, V., Pologruto, T.A., Oertner, T.G., Sabatini, B.L., Svoboda, K., 2004. Imaging calcium concentration dynamics in small neuronal compartments. Sci. STKE 2004, l5. https://doi.org/10.1126/stke.2192004pl5.
Zelles, T., Boyd, J.D., Hardy, A.B., Delaney, K.R., 2006. Branch-specific Ca2+ influx from Na+-dependent dendritic spikes in olfactory granule cells. J. Neurosci. 26, 30–40. https://doi.org/10.1523/JNEUROSCI.1419-05.2006.
Zheng, J., Dai, C., Steyger, P.S., Kim, Y., Vass, Z., Ren, T., Nuttall, A.L., 2003. Vanilloid receptors in hearing: altered cochlear sensitivity by vanilloids and expression of TRPV1 in the organ of corti. J. Neurophysiol. 90, 444–455. https://doi.org/10.1152/jn.00919.2002.